

# On-POM ring-opening polymerisation of *N*-Carboxyanhydrides

Héctor Soria-Carrera, Isabel Franco-Castillo, Pilar Romero, Santiago Martín, Jesús M. de la Fuente, Scott G. Mitchell,\* Rafael Martín-Rapún\*

**Abstract:** The ring-opening polymerisation of  $\alpha$ -amino acid *N*-carboxyanhydrides (NCAs) offers a simple and scalable route to polypeptides with predicted and narrow molecular weight distributions. Here we show how polyoxometalates (POMs) – redox-active molecular metal-oxide anions – can serve as inorganic scaffold initiators for such NCA polymerisations. This “*On-POM polymerisation*” strategy serves as an innovative platform to design hybrid materials with additive or synergistic properties stemming from the inorganic and polypeptide component parts. We have used this synthetic approach to synthesise a library of bactericidal poly(lysine)-POM hybrid derivatives that can be used to prevent biofilm formation. This versatile “*On-POM polymerisation*” method provides a flexible synthetic approach for combining inorganic scaffolds with amino acids, and the potential to tailor and improve the specificity and performance of hybrid antimicrobial materials.

Polypeptides are ubiquitous in Nature and perform crucial roles in signalling, protecting and transport in living organisms. Most often, synthetic polypeptides are obtained by biosynthesis or by means of Solid Phase Peptide Synthesis (SPPS), which reproduce the exact peptide sequence. However, the scalability of these processes remains challenging.<sup>[1]</sup> In contrast, the Ring Opening Polymerisation (ROP) of *N*-carboxyanhydrides (NCAs) has emerged as an atom efficient one-pot route to polypeptides under living polymerisation conditions.<sup>[2,3]</sup> This approach allows the scalable synthesis of peptidomimetics that gather the main features needed for a certain function such as charge, hydrophilicity/hydrophobicity or secondary structure. Thus, its use has been explored with different naturally occurring amino acid monomers and initiators to confer specific functionality and different chemistries to the peptidic chain.<sup>[4–6]</sup> In addition to conventional initiators as organic nucleophiles, several non-conventional platforms such as gold surfaces or metallic nanoparticles have been employed as NCA polymerisation

initiators.<sup>[7–9]</sup> The surface-initiated ROP of NCAs relies on the immobilisation of amino groups at the surface that can initiate the polymerisation. This attractive concept combines the robustness of a metallic support with the high functionality of polypeptides. Although the controlled binding and assembly of polypeptides onto inorganic substrates lies at the core of biological-materials engineering, these scaffolds are not discrete molecules and mostly comprise noble metals, minerals or metal-oxides such as hydroxyapatite, calcite, magnetite and silica.

Polyoxometalates (POMs) are molecular metal-oxides with elevated redox activity that have been employed in fields as diverse as catalysis, energy and biology.<sup>[10–12]</sup> These cluster anions can be easily tuned to tailor the physicochemical properties for a variety of applications by varying the number and/or type of metal addenda atom or introducing organic ligands. Organic hybrids of POMs offer versatile platforms to develop new materials that potentially combine the properties of both entities.<sup>[13–15]</sup> In particular, the well-known Mn-Anderson derivative can be functionalised with Tris-base producing bis-amino functionalised POM  $[\text{MnMo}_6\text{O}_{18}((\text{OCH}_2)_3\text{CNH}_2)_2]^{3-}$  for post-reaction development.<sup>[16,17]</sup> Cronin and co-workers paved the way towards hybrid-POM-peptidic composites via covalent attachment<sup>[18]</sup> or introducing them in a SPPS-like workflow.<sup>[19]</sup> Further, POMs have been also derivatised in such a way that they act as initiators of radical polymerisations<sup>[20,21]</sup> or as repeating unit in a polymer sequence.<sup>[22,23]</sup>

POMs have been shown to exhibit antimicrobial properties arising from their redox properties and their interaction with bacterial cell membranes, which results in membrane puncturing and cell lysis.<sup>[24]</sup> Antimicrobial peptides (AMPs) have received increasing attention because of their rapid action and broad-spectrum antimicrobial activities. They are usually formed by sequences combining hydrophobic and cationic amino acids. The dual functionality arising from these cationic and amphiphilic properties allows AMPs to attach to the anionic microbial cell membranes, intercalate into the lipid bilayers and eventually disrupt the cell membrane.<sup>[25]</sup> Importantly, libraries of AMPs can easily be prepared by ROP of NCAs.<sup>[26–28]</sup>

Since both POMs and polypeptides have each been shown to exhibit potent antimicrobial properties, it therefore follows that hybrid materials based on these components emerge as interesting candidates to overcome the increasing problem of bacterial resistance towards conventional antibiotics.<sup>[29–32]</sup> The ionic combination of peptides or peptide-polymers and POMs have resulted in hybrids with better antimicrobial activities than each component alone.<sup>[33–35]</sup> In addition, the vast combinatorial possibilities of both POMs and amino acids means that it is also possible to tune the secondary structure, molecular weight and antimicrobial properties of the hybrid.

Here we present the use of an amino-functionalised Mn-Anderson-POM as an initiator for the on-POM ROP of amino acid NCAs. We have termed the hybrid POM-peptides obtained by this polymerisation approach as POMlymers (Figure 1). In this proof-of-principle report we combine hydrophobic (*N*<sup>ε</sup>-protected lysine)

[\*] H. Soria-Carrera, I. Franco-Castillo, Dr. P. Romero, Dr. S. Martín, Prof. J. M. de la Fuente, Dr. S. G. Mitchell, Dr. R. Martín-Rapún Instituto de Nanociencia y Materiales de Aragón (INMA) CSIC-Universidad de Zaragoza

c/ Pedro Cerbuna 12, 50009 Zaragoza (Spain)

E-mail: [scott@unizar.es](mailto:scott@unizar.es), [rmartin@unizar.es](mailto:rmartin@unizar.es)

[b] H. Soria-Carrera, I. Franco-Castillo, Prof. J. M. de la Fuente, Dr. S. G. Mitchell, Dr. R. Martín-Rapún

CIBER de Bioingeniería, Biomateriales y Nanomedicina Instituto de Salud Carlos III

28029 Madrid (Spain)

[c] Dr. R. Martín-Rapún Departamento de Química Orgánica, Facultad de Ciencias Universidad de Zaragoza

c/ Pedro Cerbuna 12, 50009 Zaragoza (Spain)

[d] Dr. S. Martín Departamento de Química Física, Facultad de Ciencias Universidad de Zaragoza

c/ Pedro Cerbuna 12, 50009 Zaragoza (Spain)

Supporting information [containing full characterisation data](#) for this article is given via a link at the end of the document.

## COMMUNICATION

and cationic residues (lysine) to explore the antimicrobial and antibiofilm behaviour of the resulting POMlymers. To the best of our knowledge, this is the first example of ROP using a molecular metal-oxide as initiator and inorganic molecular scaffold. From a fundamental standpoint, this “on-POM polymerisation” strategy represents a modular and controllable synthetic approach for producing libraries of POMlymers with controlled molecular weight and structure, from organo-functionalised POMs and amino acids. Such an approach could pave the way to next generation hybrid materials with additive or synergistic antimicrobial properties.

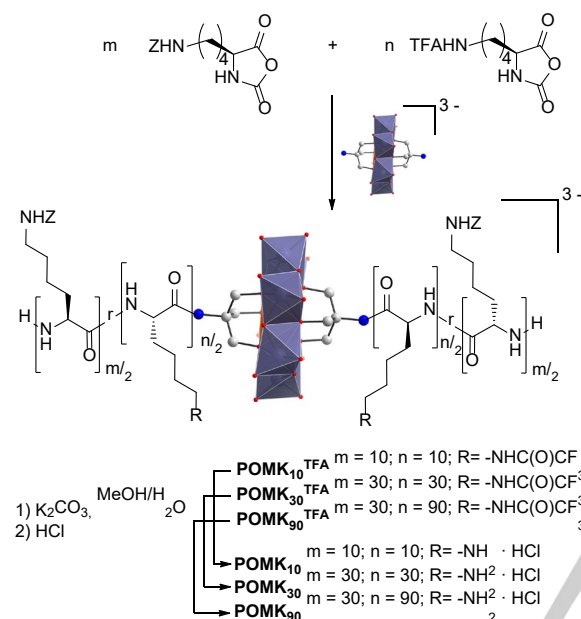


**Figure 1.** On-POM preparation of POMlymers  $POMK_n^{TFA}$  via ring-opening polymerisation (ROP) of *N*-carboxyhydride (NCA) and subsequent deprotection to obtain the positively charged POMlymers  $POMK_n$ .

ZK NCA and TFAK NCA (*N*-benzyloxycarbonyl and trifluoroacetamide protected lysine respectively) were selected as precursor monomers to obtain respectively the hydrophobic and cationic residues in the final POMlymers, whereas  $[MnMo_6O_{18}((OCH_2)_3CNH_2)_2]^{3-}$  with tetrabutylammonium (TBA) as counterions was chosen as bifunctional initiator (Figure 1). To mimic the favoured structure of an AMP, we randomly copolymerised both monomers. We anticipated that the higher number of TFAK residues (lysine residues after deprotection) would confer a higher degree of antimicrobial activity due to the increased number of cationic residues. In consequence, we fixed the hydrophobic residue content at 30 repeating units and we set the TFAK NCA feed to 30 and 90 residues ( $POMK_{30}^{TFA}$  and  $POMK_{90}^{TFA}$ ). We also prepared a short oligomer containing 10 residues of each monomer,  $POMK_{10}^{TFA}$ , to test whether the solubility would play an important role in the antimicrobial activity (Figure 1). As control, the synthesis of the polymers  $K_n^{TFA}$  without the POM moiety was initiated with *n*-butylamine. In all cases the polymerisation was performed following an adapted protocol that had previously ensured a living chain growth polymerisation with fast reaction kinetics by removing the  $CO_2$  formed during the reaction.<sup>[36,37]</sup> All the polymers could be isolated by precipitation in either water or diethyl ether. In the case of POMlymers,

precipitation in water offered the advantage that TBA cations could be removed almost completely, which was crucial in order to perfectly isolate the contributions of the POM against bacteria, since tetraalkylammonium cations are known antibacterial agents.<sup>[29]</sup>

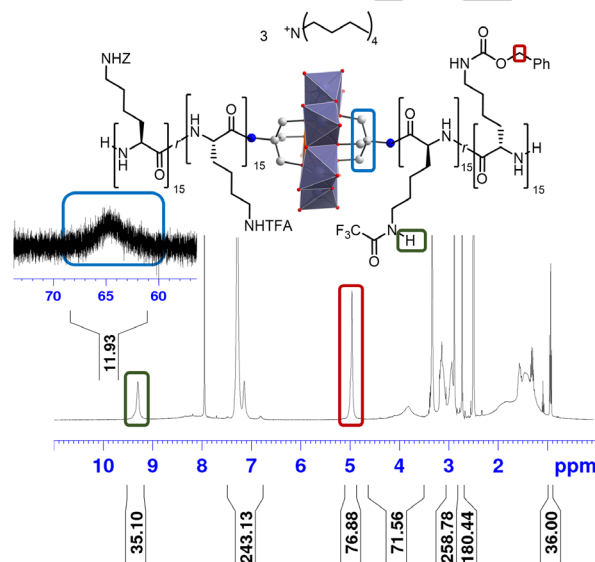


**Figure 2.** Structure of  $POMK_{30}^{TFA}$  and  $^1H$  NMR spectrum of  $POMK_{30}^{TFA}$ . Relevant signals to characterise the structure of the polymers are highlighted with colour boxes.

After polymerisation, the composition of the polymeric scaffold was evaluated using  $^1H$ -NMR on the POMlymers precipitated in diethyl ether (Figure 2 and S8-S10). The ratio between the comonomers reflected that of the reaction mixture as calculated from the integration of the proton signals of the trifluoroacetamide and the benzylic hydrogens of the Z protecting group (Figure 2). The methylene protons closer to the Mn(III) core in the Tris-functionalised POM were used to determine the average degree of polymerisation, which corresponded well with that defined by the feed (Table 1). Due to the strong paramagnetic behaviour of Mn(III) the methylene signal is subject to a large downfield chemical shift and its signal appears at ca. 65 ppm (inset in Figure 2). When precipitated in water instead of diethyl ether, TBA cations were mostly removed which led to the disappearance of the methylene signal at ca. 65 ppm. The suppression of the signal was probably due to the change in the environment of paramagnetic Mn(III) ion as well as solvation effects, as it was recovered after treating the material with a solution of TBA bromide in diethyl ether (Figure S23).

**Table 1.** Characterisation results of POMlymers  $POMK_n^{TFA}$ .

Feed <sup>[a]</sup>	$POMK_n^{TFA}$			$POMK_n$		
	$M_n^{[b]}$ [kg/mol]	Ratio <sup>[a]</sup> (NMR)	$M_n$ (NMR) <sup>[c]</sup> [kg/mol]	$M_n^{[d]}$ [kg/mol]	$M_n$ (GPC) <sup>[e]</sup> [kg/mol]	$\bar{D}$ (GPC)
10:10	6.0	1:11:11	6.5	5.1	-	-
30:30	15.7	1:38:35	19.0	12.9	21.0	1.19

30:90 29.2 1:38:89 31.0 20.6 29.3 1.35

[a] Expressed by the molar ratio POM:ZK:TFAK in the feed and in the polymer (NMR). [b] As calculated based on the feed but excluding TBA. [c] Calculated based on the integration of Tris signal at ca. 65 ppm. [d] As calculated based on the feed but excluding hydrochloride and TBA. [e] Relative to PMMA standards with HFIP with  $3 \text{ g L}^{-1} \text{ K}^+ \text{TFA}^-$  as eluent.

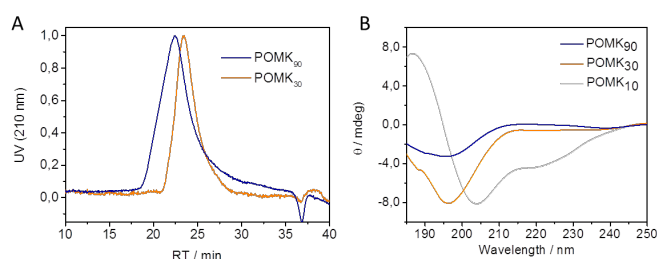


**Figure 3.** A) GPC profiles (UV absorbance at 210 nm) of POMlymers **POMK<sub>90</sub>** and **POMK<sub>30</sub>**; B) CD spectra of **POMK<sub>90</sub>**, **POMK<sub>30</sub>** and **POMK<sub>10</sub>** as measured in HFIP ( $0.1 \text{ mg L}^{-1}$ ).

The targeted materials (POMK<sub>n</sub>) were prepared by selective cleavage of the trifluoroacetamide group under mild alkaline conditions.<sup>[38]</sup> The successful cleavage was confirmed by the disappearance of the  $-\text{CF}_3$  signal in  $^{19}\text{F}$ -NMR (Figure S22). The materials were insoluble in DMSO and  $\text{H}_2\text{O}$ , nevertheless, it was possible to solubilise them with hexafluoroisopropanol (HFIP), which is known to favour the dissolution of hydrogen bonded aggregates.  $^1\text{H}$ -NMR spectra of **POMK<sub>n</sub>** showed only signals belonging to the polypeptidic chain and side groups while the methylene signals of Tris ligands were suppressed (Figures S12-S14). POM decomposition or fragmentation during the deprotection step would give rise to a broader variety of polymeric structures with smaller size. In consequence we used DOSY (Diffusion Ordered Spectroscopy)  $^1\text{H}$ -NMR as a tool to determine whether the POM was still attached to the polypeptide. **POMK<sub>n</sub><sup>TFA</sup>** and **POMK<sub>n</sub>** showed that the presence of the paramagnetic Mn(III) not only affects the signal of the Tris methylene protons but also the signals along the polymeric structure, mainly  $\alpha$ -protons: After applying the magnetic field gradients, the methylene bridges in Tris ligands and the  $\alpha$ -proton signals were suppressed due to the interaction with the magnetic field. This effect seems to be more pronounced for **POMK<sub>n</sub><sup>TFA</sup>** than for **POMK<sub>n</sub>**. However, in polymers **K<sub>n</sub><sup>TFA</sup>** and **K<sub>n</sub>**, without POM, we did not observe this phenomenon, confirming that the paramagnetic effect is indeed transferred through the peptide backbone. When comparing DOSY spectra of both **POMK<sub>n</sub>** and **K<sub>n</sub>** polymers we did not observe any significant change on the pattern of the molecular diffusion (Figure S24-S29), concluding that the POM was still attached to the polymer in **POMK<sub>n</sub>**. Additionally, the presence of the POM was verified directly by using a combination of FTIR (Figures S31-S33) and X-ray Photoelectron Spectroscopy (XPS) (Figures S37-S38). Briefly, FTIR spectra can be used to prove the presence of Mn-Anderson  $[\text{MnMo}_6\text{O}_{18}(\text{OCH}_2)_3\text{CNH}_2)_2]^{3-}$  in the final **POMK<sub>n</sub>** materials. The Mo=O and Mo-O stretches (ca.  $890 \text{ cm}^{-1}$  and  $690 \text{ cm}^{-1}$ , respectively) are present for MnMo<sub>6</sub> Mn-Anderson starting material and **POMK<sub>n</sub>**. These bands are absent in **K<sub>n</sub>**, which do not contain the MnMo<sub>6</sub> Mn-Anderson, showing that the bands in the  $1200\text{-}600 \text{ cm}^{-1}$  region of the spectra in the final **POMK<sub>n</sub>** materials

do not correspond to the peptidic part. (Figures S31-S33). XPS was used to identify Mn(III) and Mo(VI) in **POMK<sub>n</sub>** POMlymers.

Consistent with the DOSY spectra, gel permeation chromatography traces recorded for **POMK<sub>n</sub>** in HFIP with  $3 \text{ g L}^{-1} \text{ K}^+ \text{TFA}^-$  showed monomodal distributions for POMlymers **POMK<sub>90</sub>** and **POMK<sub>30</sub>**, with estimated molecular weights similar to the control polymers **K<sub>90</sub>** and **K<sub>30</sub>**. **POMK<sub>10</sub>** exhibited scarce solubility and therefore its GPC was not measured.

Bearing in mind the importance of conformational structure for developing materials with antimicrobial properties, we used circular dichroism (CD) spectroscopy to study the differences in how the polypeptide sequence folds (in HFIP) when conjugated to the POM. For the shortest POMlymer (**POMK<sub>10</sub>**) we observed that the metallic centre favoured the folding into  $\alpha$ -helices (Figure 3), in turn, its analogue **K<sub>10</sub>** did not show any particular conformation but random coil (Figure S34). This phenomenon was already described by Yvon and Ventura *et al.*, for POM and peptide hybrids prepared by SPPS, but without any further explanation.<sup>[19,39]</sup> In contrast, **POMK<sub>30</sub>** and **POMK<sub>90</sub>** adopted a random coil conformation whereas their POM-free counterparts **K<sub>30</sub>** and **K<sub>90</sub>** formed  $\alpha$ -helices (Figures 3B and S34). Our hypothesis is that POM-free structures possess a longer uninterrupted peptide chain, with a larger number of ZK residues which are known to induce a helical conformation. However, when the solvent contained  $3 \text{ g L}^{-1} \text{ K}^+ \text{TFA}^-$  as used in GPC,  $\alpha$ -helices were detected for all POMlymers **POMK<sub>n</sub>** and control polymers **K<sub>n</sub>**, even for **K<sub>10</sub>** (Figures S35-S36). It therefore follows that **K<sub>10</sub>** should be less prone to adopting the  $\alpha$ -helix conformation and would lead to the coexistence of  $\alpha$ -helix and random coil conformations in HFIP containing  $3 \text{ g L}^{-1} \text{ K}^+ \text{TFA}^-$ . This is translated to an apparent bimodal GPC trace and broader molecular weight distribution (Table S1 and Figure S30).<sup>[40]</sup>

**Table 2.** Surface antimicrobial activity of **POMK<sub>10</sub>** and **POMK<sub>90</sub>** determined using the Japanese Industrial Standard (JIS Z 2801).

Sample	Concentration [ $\mu\text{g cm}^{-2}$ ]	Bacterial reduction [%]
<b>POMK<sub>10</sub></b>	640	100
	160	100
	20	41
<b>POMK<sub>90</sub></b>	640	100
	160	100
	20	100

[a] Refer to Figure S43 for full log(CFU) reduction data.

The presence of poly(lysine) combined with the limited aqueous solubility make POMlymers interesting candidates for antimicrobial surface coatings to prevent biofilm formation.<sup>[25,41]</sup> Bacteria that attach to a surface or to an interface can grow as a densely packed multicellular community of microorganisms, a biofilm, that protect them from the bactericidal effects of different antimicrobials, such as antibiotics. Biofilms are the source of persistent infections of many pathogenic microbes. The



POMlymers in this report were evaluated against the Gram-positive *Bacillus subtilis*, which is a widely studied non-pathogenic biofilm model.<sup>[42,43]</sup> Colorimetric cell viability assays were used to determine the bactericidal activity of the POMlymers (expressed as the concentration of the POMlymer per cm<sup>2</sup>). The bactericidal activity of **POMK<sub>90</sub>** against *B. subtilis* corresponded to 31.2 µg cm<sup>-2</sup>, while the bactericidal concentration of **POMK<sub>10</sub>** was 500 µg cm<sup>-2</sup> (Figure S39). As control experiments, we also evaluated each counterpart individually and the combination of K<sub>n</sub> with Na<sub>3</sub>[MnMo<sub>6</sub>O<sub>18</sub>((OCH<sub>2</sub>)<sub>3</sub>CNH<sub>2</sub>)<sub>2</sub>]<sup>[44]</sup> (Figures S40-S42). All antibacterial results are summarized in Table S2.

The surface antibacterial activity was also confirmed using a modified Japanese Industrial Standard (JIS Z 2801), which verified that **POMK<sub>90</sub>** provided a complete bacterial cell viability reduction on surfaces at concentrations as low as 20 µg cm<sup>-2</sup> (Table 2). **POMK<sub>10</sub>** provided surface bactericidal action at concentrations of 640 and 160 µg cm<sup>-2</sup> while at lower concentrations of 20 µg cm<sup>-2</sup> the bacterial reduction was determined to be 41 % (please also refer to Figure S43 for log(CFU) reduction data).

and by Crystal Violet assays. The ESEM analysis of the biofilm growth over silicon wafers (coated with different concentrations of the POMlymers) showed how *B. subtilis* colonised the non-coated sample and developed a biofilm, while the coated samples fully inhibit biofilm development (Figure 4). Both **POMK<sub>10</sub>** and **POMK<sub>90</sub>** fully protect from *B. subtilis* surface colonisation; however, some bacteria aggregates were observed in the 20 µg cm<sup>-2</sup> **POMK<sub>10</sub>** sample, commensurate with the antimicrobial results (Figure S43). A Crystal Violet assay, on the other hand, was used to evaluate the ability of the bacteria to develop a pellicle biofilm at the liquid-air interface. Spectrophotometric analysis of the intensity of the biofilm halo developed at the liquid-air interface demonstrated that both **POMK<sub>90</sub>** and **POMK<sub>10</sub>** inhibit biofilm formation at concentrations as low as 160 µg cm<sup>-2</sup> (Figure S44).

In this work we have demonstrated how hybrid POM-materials can be accessed through ring opening polymerisation (ROP) of *N*-carboxyanhydrides (NCAs) where the POM serves as the molecular metal-oxide scaffold initiator. We have termed the hybrid POM-peptides prepared using this approach as POMlymers. Here we have shown how a series of poly(lysine)-functionalised POMs were prepared under living polymerisation conditions by varying the number of cationic residues and the length of the polymer and that after the deprotection step in basic medium, the integrity of the POM is preserved. Some of these bactericidal POMlymers possessed surface antibacterial activity at concentrations as low as 20 µg cm<sup>-2</sup> (**POMK<sub>90</sub>**), which completely prevent biofilm growth. The **POMK<sub>90</sub>** POMlymer serves as a promising proof-of-concept candidate whose design could be improved to develop new antimicrobial hybrids to inhibit a range of biofilms that provide highly protective environments to pathogenic bacteria. The combination potential of both POMs and peptides is vast and so the broad scope of the *on-POM polymerisation* as a versatile route to produce new hybrid materials opens the door to new design principles for improving the performance of the materials to tackle biofilms that are highly resistant to conventional therapies.

## Acknowledgements

Financial support from Ministerio de Ciencia Innovación y Universidades (Spain) through a Ramón y Cajal fellowship (RMR, RYC-2013-12570) and Proyectos I+D+i (PID2019-109333RB-I00, PGC2018-097583-B-I00, and PID2019-105881RB-I00) and CSIC i-Link+2019 project (LINK20270). HSC and IFC are grateful for predoctoral fellowships from Ministerio de Educación Cultura y Deporte (FPU program) and Gobierno de Aragón, respectively. Further financial support from Fondo Social Europeo-Gobierno de Aragón (E15\_20R, E47\_20R and LMP33-18) and CIBER-BBN is gratefully acknowledged. The authors would like to acknowledge the Laboratorio de Microscopias Avanzadas (LMA) at Universidad de Zaragoza for offering access to their instruments and expertise, especially Guillermo Antorrena for the XPS measurements; the use of the Unidad de Apoyo a la Investigación del CEQMA (CSIC-Universidad de Zaragoza); and technical and human support provided by SGIker (UPV/EHU/ ERDF, EU). The authors also thank Dr. Elena Atrián-Blasco for fruitful discussions.

**Figure 4.** Environmental Scanning Electron Microscopy (ESEM) images of *B. subtilis* incubated over a silicon wafer coated with **POMK<sub>10</sub>** and **POMK<sub>90</sub>** at 20 and 640 µg cm<sup>-2</sup> (and over a non-coated sample as a biofilm positive control). Bacteria incubated over the non-coated sample are covering the surface by developing a biofilm. Some bacterial aggregates in the sample coated with 20 µg cm<sup>-2</sup> **POMK<sub>10</sub>**, but at the highest concentration (640 µg cm<sup>-2</sup>) no bacteria were observed. Surfaces coated with 20 or 640 µg cm<sup>-2</sup> **POMK<sub>90</sub>** show no biofilm growth.

The biofilm prevention properties of the POMlymers were also studied by Environmental Scanning Electron Microscopy (ESEM)

Keywords: Polypeptides • Polyoxometalates • Ring Opening Polymerisation • Antimicrobial activity • Biofilm

- [1] J. M. Palomo, *RSC Adv.* **2014**, *4*, 32658–32672.
- [2] H. R. Kricheldorf, *Angew. Chemie - Int. Ed.* **2006**, *45*, 5752–5784.
- [3] J. H. Vrijssen, A. Rasines Mazo, T. Junkers, G. G. Qiao, *Macromol. Rapid Commun.* **2020**, *2000071*, 1–6.
- [4] T. J. Deming, *Chem. Rev.* **2016**, *116*, 786–808.
- [5] O. Zagorodko, J. J. Arroyo-Crespo, V. J. Nebot, M. J. Vicent, *Macromol. Biosci.* **2017**, *17*, 1–22.
- [6] D. Huesmann, K. Klinker, M. Barz, *Polym. Chem.* **2017**, *8*, 957–971.
- [7] S. H. Wibowo, A. Sulistio, E. H. H. Wong, A. Blencowe, G. G. Qiao, *Chem. Commun.* **2014**, *50*, 4971–4988.
- [8] S. H. Wibowo, E. H. H. Wong, A. Sulistio, S. N. Guntari, A. Blencowe, F. Caruso, G. G. Qiao, *Adv. Mater.* **2013**, *25*, 4619–4624.
- [9] G. Marcelo, A. Muñoz-Bonilla, J. Rodríguez-Hernández, M. Fernández-García, *Polym. Chem.* **2013**, *4*, 558–567.
- [10] D. Gao, R. Liu, J. Biskupek, U. Kaiser, Y. F. Song, C. Streb, *Angew. Chemie - Int. Ed.* **2019**, *58*, 4644–4648.
- [11] D. L. Long, R. Tsunashima, L. Cronin, *Angew. Chemie - Int. Ed.* **2010**, *49*, 1736–1758.
- [12] A. Bijelic, M. Aureliano, A. Rompel, *Angew. Chemie - Int. Ed.* **2019**, *58*, 2980–2999.
- [13] A. Proust, B. Matt, R. Villanneau, G. Guillemot, P. Gouzerh, G. Izzet, *Chem. Soc. Rev.* **2012**, *41*, 7605–7622.
- [14] K. Kastner, A. J. Kibler, E. Karjalainen, J. A. Fernandes, V. Sans, G. N. Newton, *J. Mater. Chem. A* **2017**, *5*, 11577–11581.
- [15] A. V Anyushin, A. Kondinski, T. N. Parac-Vogt, *Chem. Soc. Rev.* **2020**, *49*, 382–432.
- [16] P. R. Marcoux, B. Hasenknopf, J. Vaissermann, P. Gouzerh, *Eur. J. Inorg. Chem.* **2003**, 2406–2412.
- [17] A. Blazevic, A. Rompel, *Coord. Chem. Rev.* **2016**, *307*, 42–64.
- [18] J. Luo, B. Zhang, C. Yvon, M. Hutin, S. Gerislioglu, C. Wesdemiotis, L. Cronin, T. Liu, *Eur. J. Inorg. Chem.* **2019**, *2019*, 380–386.
- [19] C. Yvon, A. J. Surman, M. Hutin, J. Alex, B. O. Smith, D. L. Long, L. Cronin, *Angew. Chemie - Int. Ed.* **2014**, *53*, 3336–3341.
- [20] B. Hu, C. Wang, J. Wang, J. Gao, K. Wang, J. Wu, G. Zhang, W. Cheng, B. Venkateswarlu, M. Wang, et al., *Chem. Sci.* **2014**, *5*, 3404–3408.
- [21] Y. Han, Y. Xiao, Z. Zhang, B. Liu, P. Zheng, S. He, W. Wang, *Macromolecules* **2009**, *42*, 6543–6548.
- [22] W. K. Miao, Y. K. Yan, X. Le Wang, Y. Xiao, L. J. Ren, P. Zheng, C. H. Wang, L. X. Ren, W. Wang, *ACS Macro Lett.* **2014**, *3*, 211–215.
- [23] W. K. Miao, A. Yi, Y. K. Yan, L. J. Ren, D. Chen, C. H. Wang, W. Wang, *Polym. Chem.* **2015**, *6*, 7418–7426.
- [24] A. Bijelic, M. Aureliano, A. Rompel, *Chem. Commun.* **2018**, *54*, 1153–1169.
- [25] Q. Gao, P. Li, H. Zhao, Y. Chen, L. Jiang, P. X. Ma, *Polym. Chem.* **2017**, *8*, 6386–6397.
- [26] Y. Wu, D. Zhang, P. Ma, R. Zhou, L. Hua, R. Liu, *Nat. Commun.* **2018**, *9*, 1–10.
- [27] W. Jiang, X. Xiao, Y. Wu, W. Zhang, Z. Cong, J. Liu, S. Chen, H. Zhang, J. Xie, S. Deng, et al., *Biomater. Sci.* **2020**, *8*, 739–745.
- [28] Y. Zhang, W. Song, S. Li, D.-K. Kim, J. H. Kim, J. R. Kim, I. Kim, *Chem. Commun.* **2020**, *56*, 356–359.
- [29] A. Misra, I. Franco Castillo, D. P. Müller, C. González, S. Eyssautier-Chuine, A. Ziegler, J. M. de la Fuente, S. G. Mitchell, C. Streb, *Angew. Chemie - Int. Ed.* **2018**, *57*, 14926–14931.
- [30] A. J. Park, J. P. Okhovat, J. Kim, *Clin. Basic Immunodermatology Second Ed.* **2017**, *26*, 81–95.
- [31] M. Xiong, M. W. Lee, R. A. Mansbach, Z. Song, Y. Bao, R. M. Peek, C. Yao, L.-F. Chen, A. L. Ferguson, G. C. L. Wong, et al., *Proc. Natl. Acad. Sci.* **2015**, *112*, 13155–13160.
- [32] P. Salas-Ambrosio, A. Tronnet, P. Verhaeghe, C. Bonduelle, *Biomacromolecules* **2020**, DOI 10.1021/acs.biomac.0c00797.
- [33] L. P. Datta, R. Mukherjee, S. Biswas, T. K. Das, *Langmuir* **2017**, *33*, 14195–14208.
- [34] J. Li, Z. Chen, M. Zhou, J. Jing, W. Li, Y. Wang, L. Wu, L. Wang, Y. Wang, M. Lee, *Angew. Chemie - Int. Ed.* **2016**, *55*, 2592–2595.
- [35] S. Zhang, B. Peng, P. Xue, X. Kong, Y. Tang, L. Wu, S. Lin, *Soft Matter* **2019**, *15*, 5375–5379.
- [36] N. C. A. R. Polymerizations, J. Zou, J. Fan, X. He, S. Zhang, H. Wang, K. L. Wooley, **2013**, 17–20.
- [37] H. Soria-Carrera, A. Lucía, L. De Matteis, J. A. Aínsa, J. M. de la Fuente, R. Martín-Rapún, *Macromol. Biosci.* **2019**, *19*, 1800397.
- [38] J. R. Hernandez, H. A. Klok, *J. Polym. Sci. Part A Polym. Chem.* **2003**, *41*, 1167–1187.
- [39] D. Ventura, A. Calderan, C. Honisch, S. Krol, S. Serrati, M. Bonchio, M. Carraro, P. Ruzza, *Pept. Sci.* **2018**, *110*, e24047.
- [40] D. Huesmann, A. Birke, K. Klinker, S. Türk, H. J. Räder, M. Barz, *Macromolecules* **2014**, *47*, 928–936.
- [41] J. Hasan, R. J. Crawford, E. P. Ivanova, *Trends Biotechnol.* **2013**, *31*, 295–304.
- [42] S. Arnaouteli, C. E. MacPhee, N. R. Stanley-Wall, *Curr. Opin. Microbiol.* **2016**, *34*, 7–12.
- [43] S. Gingichashvili, D. Duanis-Assaf, M. Shemesh, J. D. B. Featherstone, O. Feuerstein, D. Steinberg, *Front. Microbiol.* **2017**, *8*, 1–9.
- [44] Z. He, B. Li, H. Ai, H. Li, L. Wu, *Chem. Commun.* **2013**, *49*, 8039–8041.

WILEY-VCH

---